Effects of Leading-edge Tubercles on the Aerodynamic Performance of Rectangular Blades for low-speed Wind Turbine Applications

Parankush Koul[1]*, Mahesh K. Varpe[2], Pritam Bhat[3], Aniket Mishra[4], Chirag Malhotra[5], Devang Kalra[6]

[1,4,5,6]Student - Department of Mechanical and Manufacturing Engineering, M.S. Ramaiah University of Applied Sciences, Bangalore, Karnataka, India

[2]Associate Professor - Department of Aerospace and Automotive Engineering, M.S. Ramaiah University of Applied Sciences, Bangalore, Karnataka, India

[3]Assistant Professor - Department of Mechanical and Manufacturing Engineering, M.S. Ramaiah University of Applied Sciences, Bangalore, Karnataka, India

***Corresponding Author Email Id:** pkoul2.iit@gmail.com

ABSTRACT

The rapid depletion of conventional energy resources like fossil fuels has harmed the environment. Hence, there is an urgent need to seek alternative and sustainable energy sources. Wind energy is considered one of the efficient sources of energy that can be converted to a useful form of electrical energy. Though the field of wind engineering has developed in recent years there is still scope for improvement in the effective utilization of energy. The turbine blades' aerodynamics and the turbulent fluid flow characteristics largely determine the wind turbine's energy efficiency. Hence, in the present studies, we investigated the improvement of small wind turbine blade design by incorporating bioinspired tubercles into blades. One of the issues of small wind turbines is the low-capacity factor in power. The wind in such circumstances under buildings and other adjacent obstructions for small turbines is normally weak, unstable, and turbulent in wind speed and direction. Thus, the design of small turbines needs to be improved to capture low wind speeds and to respond quickly to turbulent wind resource areas. Biomimetics is a science that helps us adapt designs from nature to solve modern problems. The wing-like flipper of the humpback whale (Megaptera novaeangliae) has a morphology with potential for aerodynamic applications. The humpback whale flipper has several sinusoidal rounded bumps, called tubercles which modify the flow over the blade surface, creating vortices between the tubercles. Therefore, we conducted an XFOIL analysis of symmetrical NACA airfoils and we observed that NACA0012 could produce the best lift/drag ratio. The airfoil was then validated using Computational Fluid Dynamics (CFD) analysis in which the results were found comparable to that of the published data. Finally, CFD analysis was conducted for tubercles with a different pitch-to-amplitude ratio (p/A) and the tubercled airfoil with p/A of 6 provided the best result.

Keywords: Wind Energy, Aerodynamics, Turbulence, Bioinspired Design, CFD Analysis

INTRODUCTION

The problems of global warming, environmental pollution, and energy security have increased interest in developing renewable energy sources such as wind, solar, hydropower, geothermal, hydrogen, and biomass as replacements for fossil fuels. Wind energy can be a suitable solution to the global climate change and energy crisis. Using wind power essentially eliminates emissions of harmful gases such as CO_2, SO_2, NO_x, and other harmful wastes as in traditional coal-fuel power plants or radioactive wastes in nuclear power plants. As fossil fuels are subject to price and supply instability, Wind energy dramatically reduces the dependence on fossil fuels, thus strengthening global energy security. The global wind power capacity increases by at least 40% every year and more than 80 percent of the global installations are in Europe. There has been tremendous growth in wind power all over the world during the recent three decades. So, our major focus is on non-conventional energy resources like Wind energy, a pioneer of renewable energy, which is developing very quickly all over the world [1].

Due to atmospheric pressure gradients, wind results from the movement of air. The larger the atmospheric pressure gradient, the higher the wind speed and thus, the greater the wind power that can be captured from the wind using wind energy-converting machinery. Wind energy is an important player in the world's energy market and is considered the energy of the future. Among the resources wind energy is available in plenty, has no harmful emissions during operation and less space requirements and there is provision for a clean source of energy, sustainability, compatibility with other land uses, rapid instigation of power, and Cost-effectiveness. The wind turbine is the device that converts the kinetic energy of the wind to electrical energy. Though big wind turbines and their associated wind farms have many advantages they have also challenges in aerodynamics. An increase in Reynolds number and blade flexibility are their typical effects on aerodynamics. The accuracy of its aerodynamic models of wind turbines is important for the development of wind energy. Wind energy presents several significant advantages that make it an appealing choice for renewable energy generation. Firstly, it is a clean source of energy, producing no greenhouse gas emissions or pollutants during operation, which helps mitigate climate change. Additionally, wind energy is abundant and renewable, harnessing the natural power of wind without depleting resources. The technology related to wind energy generation has advanced significantly, resulting in more efficient turbines that can operate effectively at various wind speeds [2]. Moreover, wind energy systems typically have low operating costs and require minimal maintenance compared to fossil fuel plants, making them economically viable in the long term [3]. Wind power also contributes to energy diversification, enhancing energy security and reducing reliance on imported fuels [4]. Overall, the advantages of wind energy include sustainability, reduced environmental impact, and cost-effectiveness, positioning it as a key player in the transition to a cleaner energy future.

Even though the cost of wind power has decreased dramatically over the past several decades, wind projects must be able to compete economically with conventional sources of electricity, and some locations may not be windy enough to be cost-competitive. So, Wind power generation faces several significant challenges that impact its efficiency and integration into the energy grid. Key challenges include the

intermittent and variable nature of wind, which leads to unpredictability in energy output, making power scheduling and management difficult [5]. In addition, the integration of wind power into existing power systems presents technical and operational issues, such as voltage and frequency fluctuations, which require advanced control strategies [6]. Infrastructure limitations, including the need for improved grid connection capabilities and the development of energy storage technologies, also hinder the effective deployment of wind energy [7]. Furthermore, economic considerations, such as the high initial capital expenditures and competition with traditional energy sources, pose additional barriers to the expansion of wind power generation. These multifaceted challenges necessitate ongoing research and innovation in technology and policy frameworks to ensure the sustainable growth of wind energy as a vital component of the renewable energy landscape.

Wind turbine technology has evolved remarkably over the years, establishing itself as one of the most exciting and dependable renewable energy sources available today. This advancement not only showcases innovation but also highlights our commitment to a sustainable future. It has moved very fast, since the early 1980s, from wind turbines of a few kilowatts to today's multimegawatt-sized wind turbines [8-10]. In addition to their size, the design of wind turbines has shifted from being convention-driven to being optimized for the operating regime and market environment. Wind turbine designs have evolved from fixed-speed, passively controlled systems with gearboxes to variable-speed, actively controlled systems, utilizing advanced power electronics, aerodynamics, and mechanical drivetrain designs, with or without gearboxes. Hence, the present study was undertaken to validate the baseline simulation results with already published experimental data, to analyze the effect of tubercle parameters on the aerodynamic performance of the rectangular blade, and to recommend the arrived specifications of tubercle for the given application.

Therefore, to arrive at the specifications of leading-edge protuberances of a rectangular blade for performance enhancement of wind turbines under low wind speed conditions after understanding the working mechanism of leading-edge tubercles through a literature survey [11-31] relevant to the designing of rectangular blades with and without protuberances for the wind turbine, the present study was undertaken to conduct XFOIL or 2D analysis of symmetrical NACA airfoils for finalizing rectangular blade specifications at a given Reynolds number, to validate CFD predictions with already published experimental data on baseline rectangular blade, to analyze the effect of tubercle parameters on the aerodynamic performance of the rectangular blade and finally recommend the arrived specifications of tubercle for the given application.

MATERIALS AND METHODS

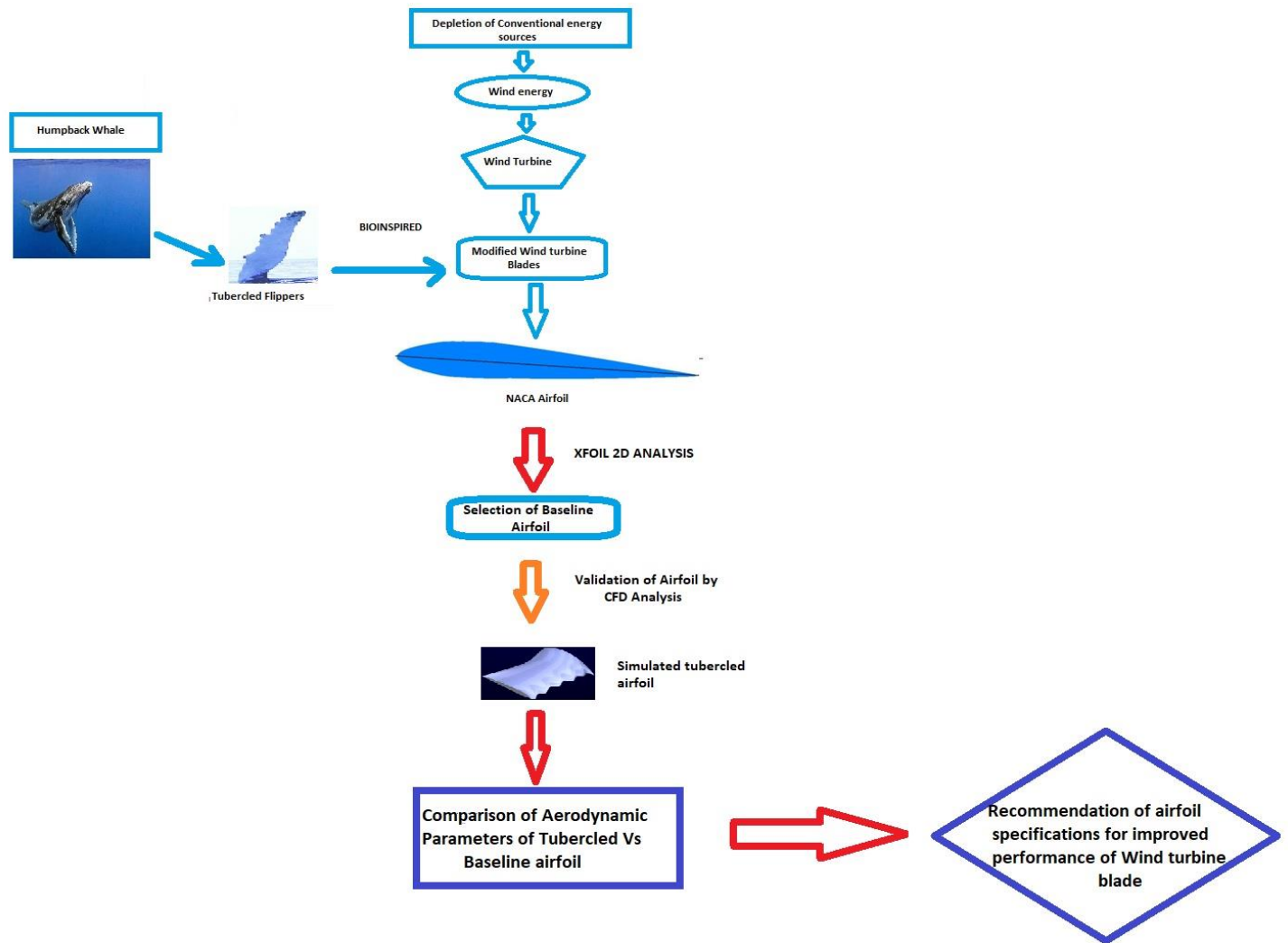Figure 1 illustrates the methodology employed in this research:

Figure 1: Methodology flowchart outlining the steps undertaken in this research

XFOIL or 2D analysis for finalizing specifications of the airfoil

XFOIL is a web-based software tool for designing and testing isolated airfoils under subsonic conditions. XFOIL version 6.99 was used to calculate pressure distribution on a 2D airfoil, lift, and drag of it with the input coordinates, Reynolds number, and Mach number.

XFOIL tool was used for the analysis of 4-digit National Advisory Committee for Aeronautics airfoils (NACA) series airfoil (NACA 0005, NACA 0010, NACA 0011, NACA 0012, NACA 0013, NACA 0014, NACA 0015, NACA 0020, NACA 0025) which are symmetrical. 4-digit NACA series airfoils were used because they have good stall characteristics, a small center of pressure movement across a large speed range, and roughness has little effect on the performance of these blades. They are used in general aviation and horizontal tails. Symmetrical airfoils were used because they have the same top and bottom faces, which lend themselves well to rotary wing applications because they have virtually no center of pressure. Travel remains almost constant across the full range of angles of attack and delivers optimal lift-drag properties for all the velocities between the rotor blade root and tip. They are used in supersonic jets, helicopter blades, shrouds, missile/rocket fins, etc.

Consider a NACA 4-digit series airfoil as: NACA MPXX

Here,

- M= Maximum camber divided by 100. For example, M=2 so the camber is 0.02 or 2% of the chord

- P= Position of the maximum camber divided by 10. For example, P=4 so the maximum camber is at 0.4 or 40% of the chord

- XX= Thickness divided by 100. For example, XX=12 so the thickness is 0.12 or 12% of the chord.

- XFOIL has capabilities for the determination of airfoil characteristics such as shape, lift, drag, and stall. XFOIL has been used by several researchers for the design and testing of airfoils.

The analysis was conducted for a Reynolds number of 50000 (lowest possible Reynolds number for the wind turbine application), Mach number of 0.13, and Ncrit (critical N-factor) value of 9. Ncrit value is used to model the turbulence of the fluid or roughness of the airfoil. The value of Ncrit was selected as 9 for average wind tunnel conditions using the following table (Table 1):

Table 1: Ncrit values and their applications

Situation	Ncrit
Sailplane	12 to 14
Motorglider	11 to 13
Clean wind tunnel	10 to 12
Average wind tunnel	9
Dirty wind tunnel	4 to 8

After XFOIL analysis, the aerodynamic performances of the airfoils were compared and the airfoil with the best performance was selected.

Validation of baseline simulation results with already published experimental data

For validation purposes, we used CFD analysis for the parameters as mentioned by Winslow et. al [32].

The software used for meshing is ICEM-CFD and the software used for simulating the meshes was ANSYS Fluent. CATIA V5 was used to make baseline 3D geometry. CATIA, an acronym of computer-aided three-dimensional interactive application, is a multi-platform software suite for computer-aided design (CAD), computer-aided manufacturing (CAM), computer-aided engineering (CAE), Product Lifecycle Management (PLM), and 3D, developed by the French company Dassault Systèmes.

The CFD solver used in this study to investigate low-Reynolds number aerodynamics is the ANSYS FLUENT and has been widely used in the past for flows past airfoil and rotor blades at high Reynolds numbers with confidence.

Validation was conducted using Winslow's experimental results of the baseline airfoil.

Analyzing the effect of tubercle parameters on the aerodynamic performance of the rectangular blade

After validation, when the simulation results were verified, the boundary conditions remained unchanged in the software for further analysis. The baseline 3D airfoil of the airfoil selected after XFOIL analysis (if different from the airfoil used in validation) was constructed using CATIA V5. The tubercles of the pitch-to-chord ratio (p/c) of 0.25 with p/As of 1, 3, 6, 9, and 12 were constructed using coordinate files containing the points of sinusoidal wave and ICEM CFD, which imported the coordinates and created the complex geometry with smoothness applicable for aerodynamic analysis. Then, ICEM CFD was used for meshing all these six geometries. These meshes (if boundary conditions were correct) were solved using ANSYS Fluent for obtaining the aerodynamic performance (lift, drag coefficients, and lift-to-drag ratio).

Recommending the arrived specifications of tubercle for the given application
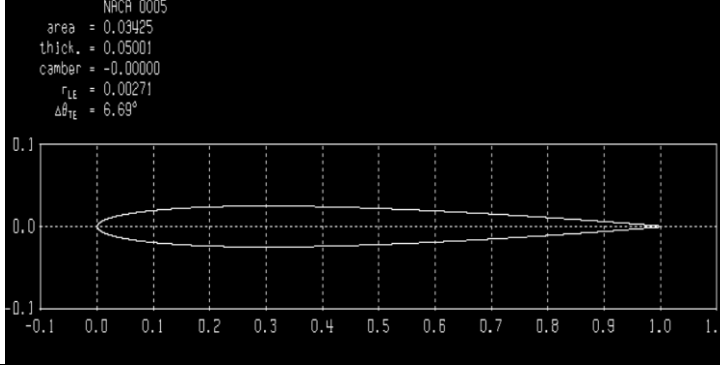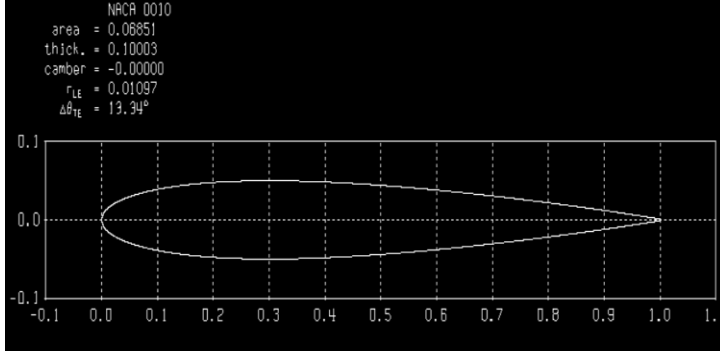
After obtaining the aerodynamic performances of all the airfoils, the performances of these airfoils were compared with each other, and the tubercled airfoil with the best performance was selected.
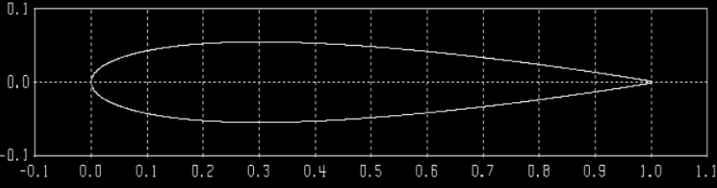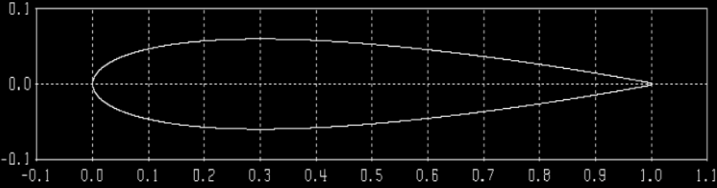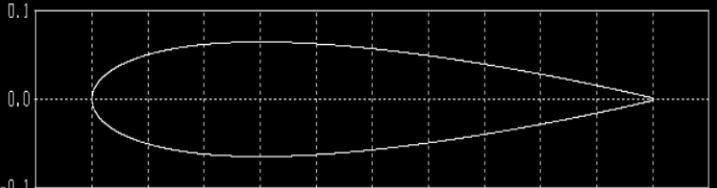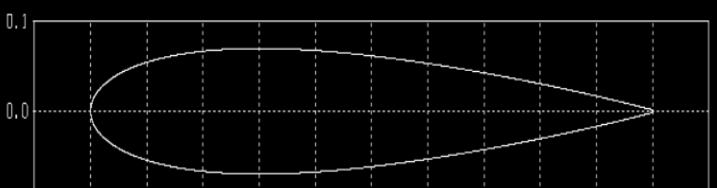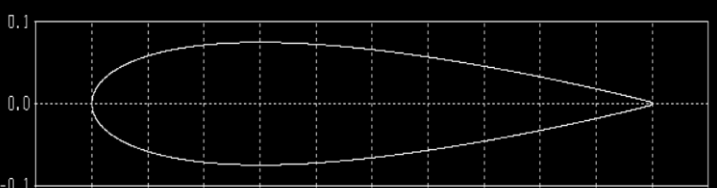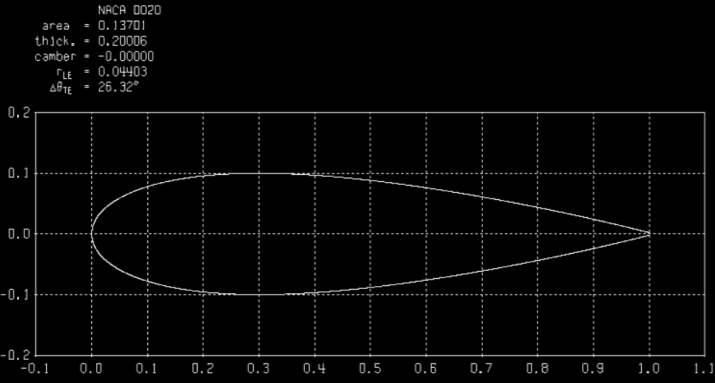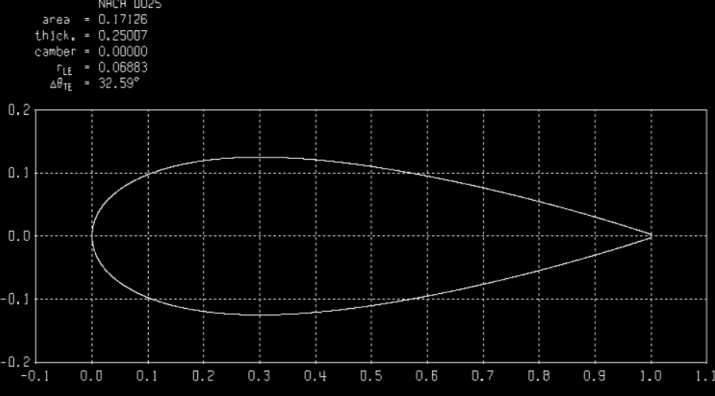
RESULTS

XFOIL-2D Analysis

The profile of the airfoils tested using XFOIL software is shown in Table 2 below:

Table 2: Results of XFOIL-2D Analysis

Airfoil Analyzed	Schematic in XFOIL	Geometric Properties
NACA 0005		Area of Airfoil= 0.03425 m^2 Thickness of Airfoil= 0.05001 m
NACA 0010		Area of Airfoil= 0.06851 m^2 Thickness of Airfoil= 0.10003 m

NACA 0011	NACA 0011 area = 0.07536 thick. = 0.11003 camber = 0.00000 r_{LE} = 0.01329 $\Delta\theta_{TE}$ = 14.66°	Area of Article =0.07536 m^2 Thickness of Airfoil =0.11003 m
NACA 0012	NACA 0012 area = 0.08221 thick. = 0.12003 camber = 0.00000 r_{LE} = 0.01582 $\Delta\theta_{TE}$ = 15.97°	Area of Airfoil= 0.08221 m^2 Thickness of Airfoil= 0.12003 m
NACA 0013	NACA 0013 area = 0.08906 thick. = 0.13004 camber = 0.00000 r_{LE} = 0.01858 $\Delta\theta_{TE}$ = 17.29°	Area of Airfoil= 0.08906 m^2 Thickness of Airfoil= 0.13004 m
NACA 0014	NACA 0014 area = 0.09591 thick. = 0.14004 camber = 0.00000 r_{LE} = 0.02155 $\Delta\theta_{TE}$ = 18.59°	Area of Airfoil= 0.09591 m^2 Thickness of Airfoil= 0.14004 m
NACA 0015	NACA 0015 area = 0.10276 thick. = 0.15004 camber = -0.00000 r_{LE} = 0.02475 $\Delta\theta_{TE}$ = 19.89°	Area of Airfoil= 0.10276 m^2 Thickness of Airfoil= 0.15004 m

| NACA 0020 | | Area of Airfoil= 0.13701 m² Thickness of Airfoil= 0.20006 m |
| NACA 0025 | | Area of Airfoil= 0.17126 m² Thickness of Airfoil= 0.25007 m |

The results obtained by simulating the above airfoils at different angle of attack (α), showing coefficient of lift (CL), coefficient of drag (CD) and lift-to-drag ratio (L/D) are as follows:

Table 3: NACA 0005 XFOIL Analysis Results

α (Degree)	CL	CD	L/D
0	0	0.01373	0
1	0.0942	0.01384	6.81
2	0.1866	0.01424	13.1
3	0.2755	0.01523	18.1
4	0.4456	0.02667	16.71
5	0.5538	0.03963	13.97
6	0.644	0.07555	8.52
7	0.6841	0.09091	7.52
8	0.6888	0.10438	6.6
9	0.6993	0.11912	5.87
10	0.7168	0.13557	5.29
11	0.731	0.15142	4.83
12	0.738	0.16464	4.48
13	0.7776	0.18559	4.19
14	0.7974	0.20027	3.98
15	0.8241	0.21602	3.81
16	0.8372	0.22181	3.77

Table 4: NACA 0010 XFOIL Analysis Results

α (Degree)	CL	CD	L/D
0	0	0.01751	0
1	0.0242	0.01815	1.33
2	0.0685	0.02024	3.38
3	0.3946	0.02168	18.2
4	0.5141	0.02053	25.05
5	0.5831	0.02353	24.79
6	0.669	0.03016	22.18
7	0.751	0.03992	18.81
8	0.7928	0.05499	14.42
9	0.7338	0.08037	9.13
10	0.6151	0.12149	5.06
11	0.6339	0.137	4.63
12	0.6432	0.15092	4.26
13	0.6663	0.16603	4.01
14	0.7071	0.18404	3.84
15	0.7106	0.19367	3.67
16	0.7367	0.2067	3.56

Table 5: NACA 0011 XFOIL Analysis Results

α (Degree)	CL	CD	L/D
0	0	0.01901	0
1	-0.0027	0.01983	-0.14
2	0.1162	0.02276	5.11
3	0.4289	0.02242	19.13
4	0.5308	0.0217	24.46
5	0.6035	0.02368	25.49
6	0.6805	0.02874	23.68
7	0.7631	0.03637	20.98
8	0.8178	0.04814	16.99
9	0.8202	0.06567	12.49
10	0.6043	0.12038	5.02
11	0.605	0.13429	4.51
12	0.6207	0.14845	4.18
13	0.6397	0.16263	3.93
14	0.6777	0.17968	3.77
15	0.6886	0.19035	3.62
16	0.7267	0.2064	3.52

Table 6: NACA 0012 XFOIL Analysis Results

α (Degree)	CL	CD	L/D
0	0	0.02098	0
1	-0.0308	0.02189	-1.41
2	0.207	0.02477	8.35
3	0.4551	0.02338	19.47
4	0.547	0.02303	23.75
5	0.6233	0.02448	25.46
6	0.6962	0.02829	24.61
7	0.7749	0.03438	22.54
8	0.8349	0.04393	19.01
9	0.8442	0.05861	14.4
10	0.6599	0.09832	6.71
11	0.5935	0.13285	4.47
12	0.6165	0.14815	4.16
13	0.6224	0.16086	3.87
14	0.6399	0.17422	3.67
15	0.6929	0.19377	3.58
16	0.6991	0.20269	3.45

Table 7: NACA 0013 XFOIL Analysis Results

α (Degree)	CL	CD	L/D
0	0	0.02358	0
1	-0.0217	0.02462	-0.88
2	0.3032	0.02613	11.61
3	0.4805	0.0245	19.62
4	0.5658	0.02437	23.21
5	0.6414	0.0257	24.95
6	0.7144	0.02864	24.94
7	0.7886	0.03353	23.52
8	0.8492	0.04135	20.54
9	0.8901	0.05212	17.08
10	0.8016	0.07262	11.04
11	0.5552	0.13059	4.25
12	0.5734	0.14482	3.96
13	0.6003	0.15952	3.76
14	0.6494	0.17735	3.66
15	0.6435	0.18563	3.47
16	0.6773	0.19938	3.4

Table 8: NACA 0014 XFOIL Analysis Results

α (Degree)	CL	CD	L/D
0	0	0.02695	0
1	0.1104	0.02808	3.93
2	0.3877	0.02708	14.32
3	0.5067	0.02582	19.63
4	0.5872	0.02578	22.78

5	0.6597	0.02713	24.32
6	0.7344	0.02943	24.96
7	0.7998	0.03373	23.71
8	0.8657	0.03971	21.8
9	0.9038	0.04907	18.42
10	0.8171	0.06753	12.1
11	0.5489	0.13099	4.19
12	0.5793	0.14652	3.95
13	0.5818	0.15794	3.68
14	0.5927	0.17009	3.48
15	0.6473	0.18876	3.43
16	0.649	0.19639	3.3

Table 9: NACA 0015 XFOIL Analysis Results

α (Degree)	CL	CD	L/D
0	0	0.0312	0
1	0.2427	0.03062	7.93
2	0.4499	0.0281	16.01
3	0.5339	0.02737	19.5
4	0.6081	0.02753	22.09
5	0.6801	0.0287	23.69
6	0.7476	0.03099	24.12
7	0.8159	0.03437	23.74
8	0.8685	0.0399	21.77
9	0.9135	0.04746	19.25
10	0.8714	0.06141	14.19
11	0.5322	0.13085	4.07
12	0.5362	0.14315	3.75
13	0.5443	0.15533	3.5
14	0.5721	0.16919	3.38
15	0.6046	0.18232	3.32
16	0.6385	0.19718	3.24

Table 10: NACA 0020 XFOIL Analysis Results

α (Degree)	CL	CD	L/D
0	0	0.04757	0
1	0.3199	0.04472	7.15
2	0.5301	0.04095	12.95
3	0.6949	0.03783	18.37
4	0.7368	0.03913	18.83
5	0.7749	0.04109	18.86
6	0.7894	0.04464	17.68
7	0.7513	0.05104	14.72
8	0.7067	0.05822	12.14
9	0.4536	0.0892	5.08
10	0.3084	0.11868	2.6
11	0.3624	0.13202	2.75
12	0.385	0.14208	2.71
13	0.3981	0.15235	2.61

14	0.4577	0.1671	2.74
15	0.4644	0.17556	2.65
16	0.4998	0.18671	2.68

Table 11: NACA 0025 XFOIL Analysis Results

α (Degree)	CL	CD	L/D
0	-0.0032	0.06497	-0.05
1	0.1258	0.06561	1.92
2	0.156	0.06879	2.27
3	0.151	0.07406	2.04
4	0.2624	0.08029	3.27
5	0.3764	0.08748	4.3
6	0.3893	0.09885	3.94
7	0.3275	0.10618	3.08
8	0.1591	0.11891	1.34
9	0.1734	0.12447	1.39
10	0.1729	0.1309	1.32
11	0.1919	0.1377	1.39
12	0.256	0.15093	1.7
13	0.2471	0.15533	1.59
14	0.2848	0.16468	1.73
15	0.3341	0.17622	1.9
16	0.391	0.19118	2.05

In this study, CL, CD and L/D obtained by XFOIL analysis at different α for different airfoils are shown in the figures below:
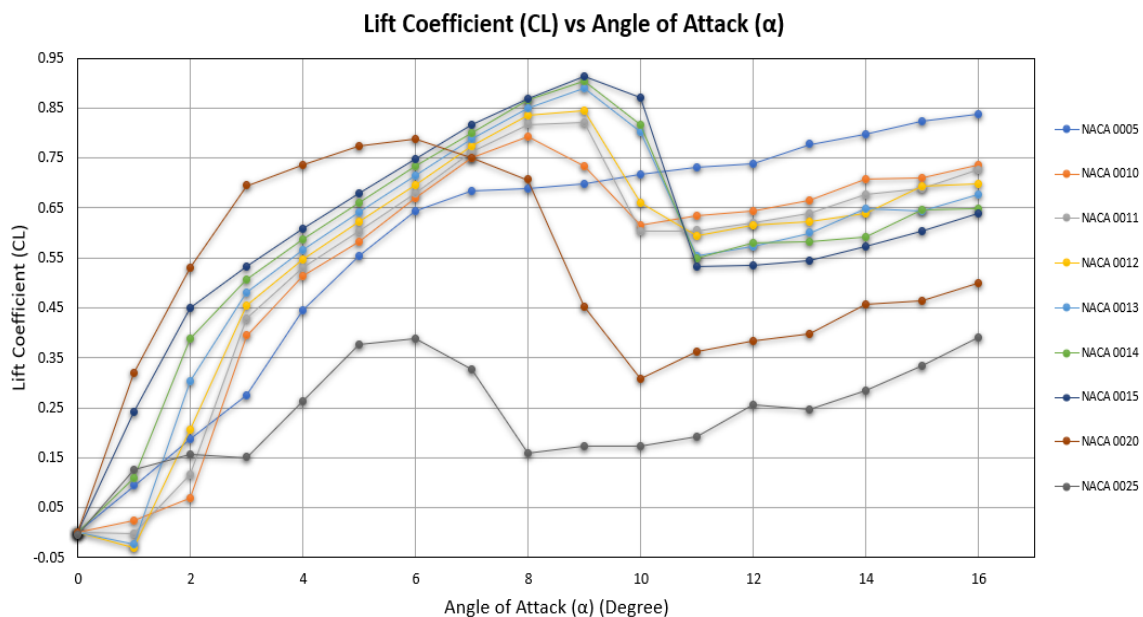

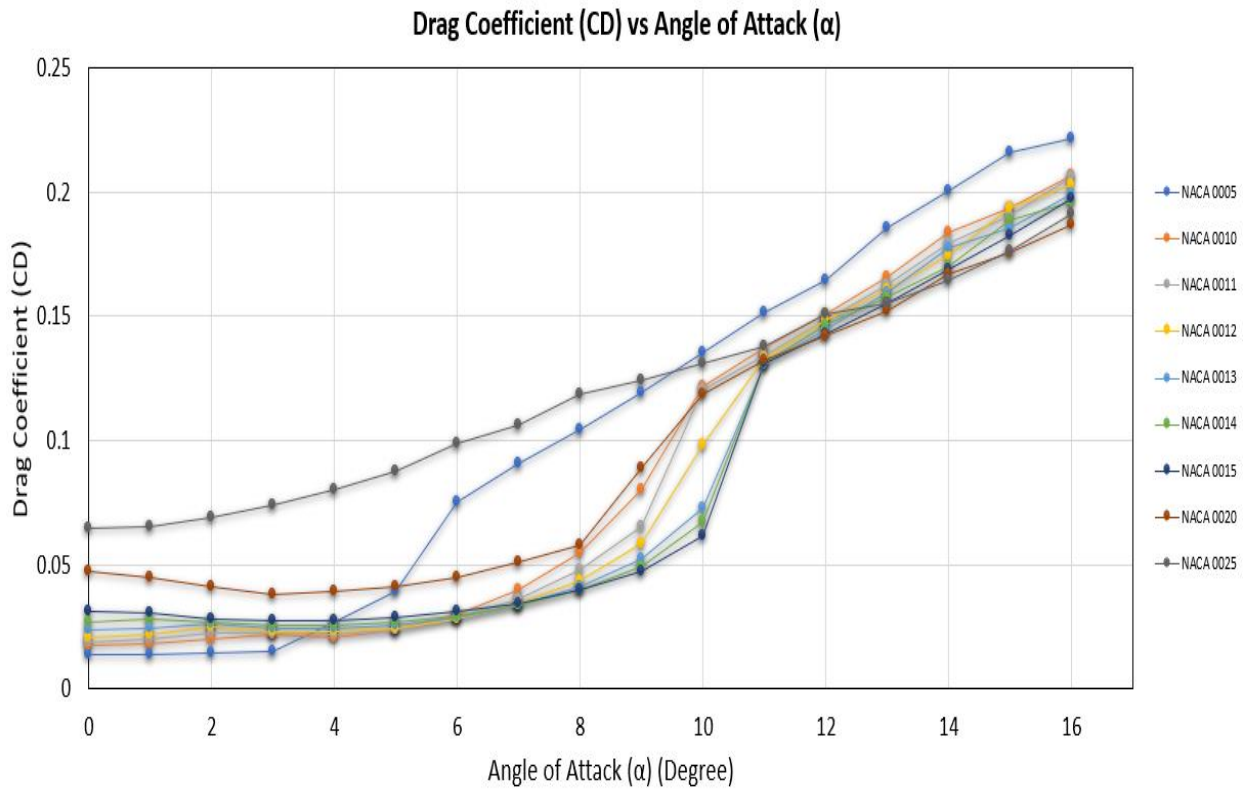**Figure 2: CL vs α (XFOIL Analysis)**

Drag Coefficient (CD) vs Angle of Attack (α)

Figure 3: CD vs α (XFOIL Analysis)

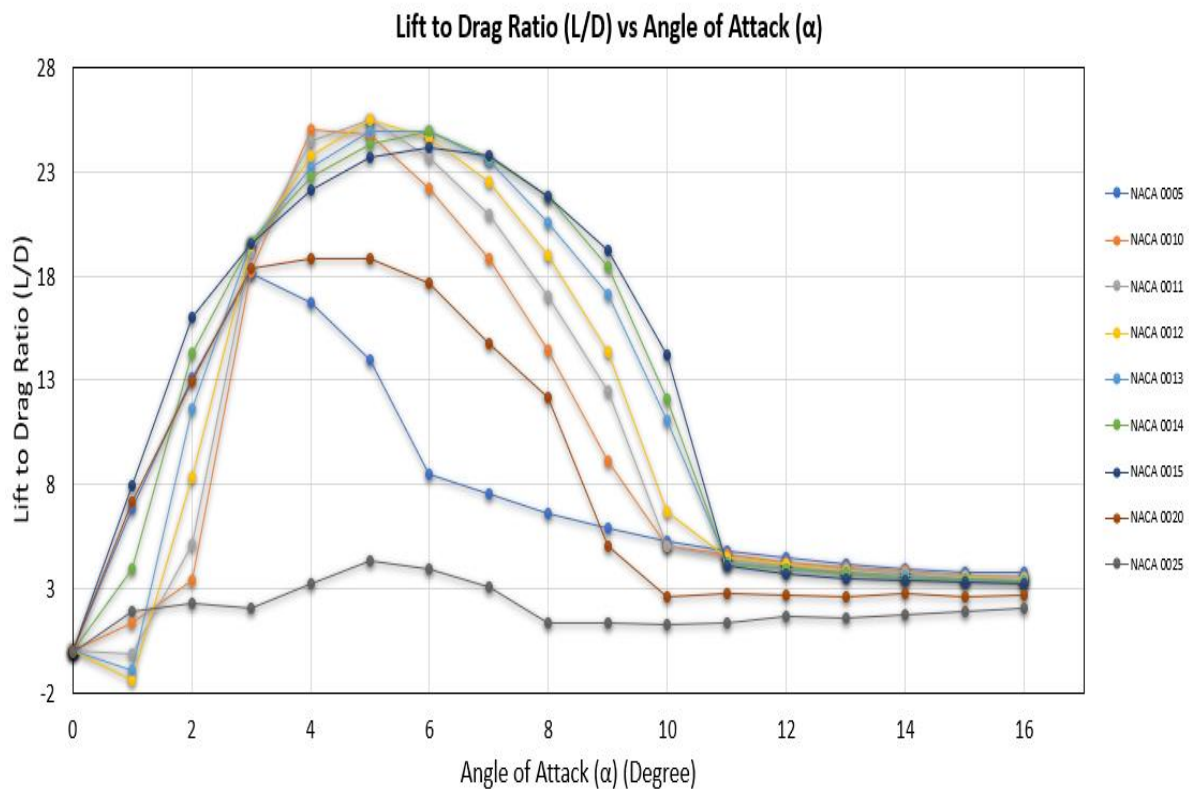### Lift to Drag Ratio (L/D) vs Angle of Attack (α)

Figure 4: L/D vs α (XFOIL Analysis)

In our investigation, XFOIL 2D analysis revealed that:

- Highest CL at stall angle: NACA 0015 (CL=0.9135) @ 9 degrees followed by NACA 0014> 0013> 0012> 0011> 0010> 0020> 0025>0005.
- NACA 0005 showed an early stalling at 3 degrees, followed by NACA 0020 and 0025 at 6 degrees, NACA 0010 at 8 degrees and other airfoils at 9 degrees.

- The drag increased with an increase in lift even after stalling because of the phenomenon known as "induced drag" or "drag due to lift". In aerodynamics, lift-induced drag, induced drag, vortex drag, or sometimes drag due to lift, is an aerodynamic drag force that occurs whenever a moving object redirects the airflow coming at it.

- In pre-stall, the CD showed a decline with a decrease in thickness from NACA 0025 to NACA 0005 and in post-stall, the CD showed a reverse effect.

- The L/Ds of NACA 0012 and 0011 were higher than that of other airfoils. However, the lift-to-drag ratios between NACA 0010 to 0015 were in the same range.

- The L/Ds of NACA 0005, 0020 and 0025 were very low compared to that of other airfoils.

- Therefore, based on the observations obtained from XFOIL analysis we selected NACA0012 airfoil for investigating the effect of leading-edge tubercles on baseline airfoil as it has the highest L/D.

CFD analysis for validation

The computational study was conducted on airfoil to simulate flows at Reynolds number at 3×10^5. The airfoil investigated in CFD analysis was NACA0012 with chord length of 1 m. The airfoil was analyzed for angle of attack ranging from 1° to 24°. The airfoil was examined for lift and drag characteristics and compared with results obtained from the experimental data of Winslow et. al for the same parameters [32]. The geometry of NACA 0012 constructed using CATIA V5 is shown in Figure 5.
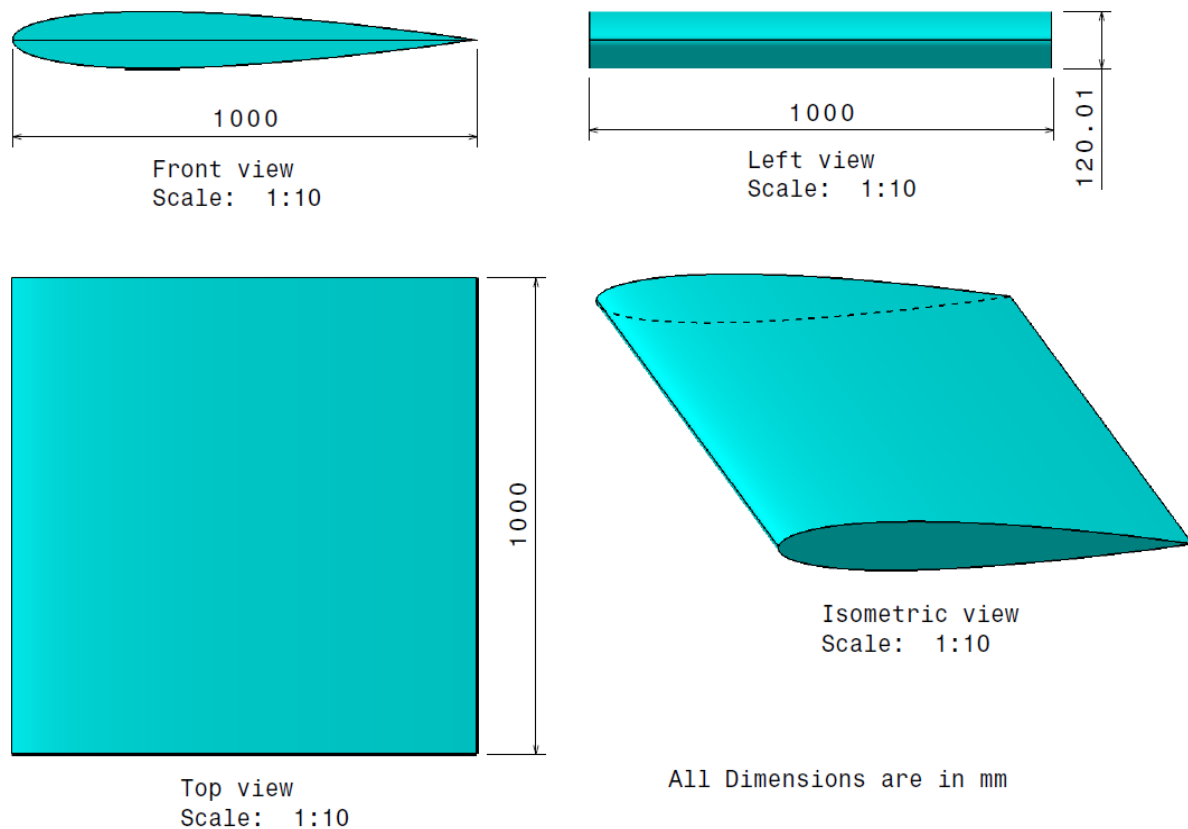

Figure 5: Geometry of NACA 0012 using CATIA V5

By importing the above geometry into ICEM CFD and meshing it using a C-type mesh, we get the following mesh:
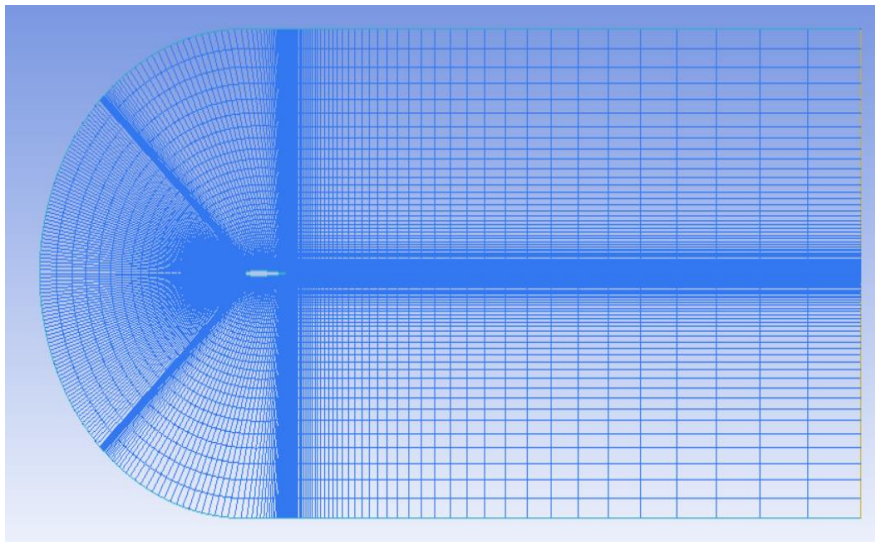
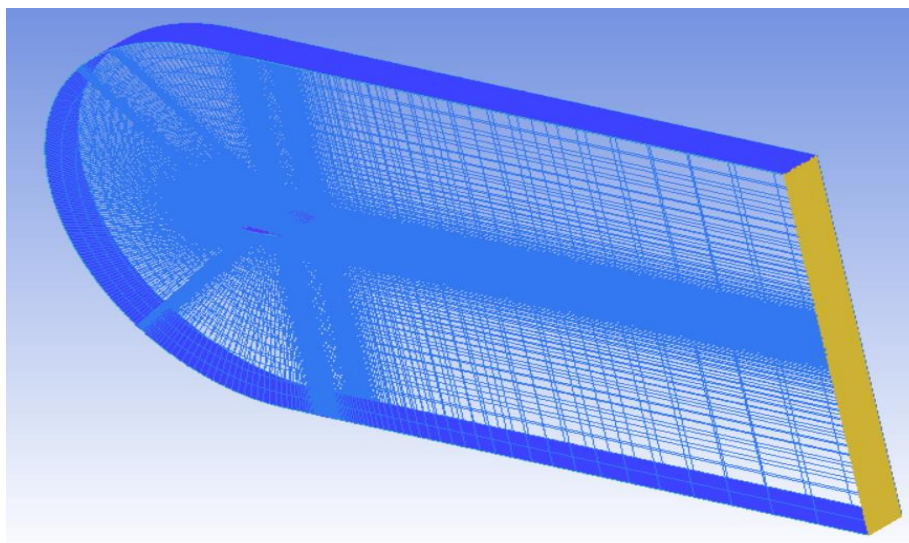**Figure 6: Side view of the mesh of baseline airfoil in ICEM CFD**

Figure 7: 3D view of the mesh of baseline airfoil with in ICEM CFD
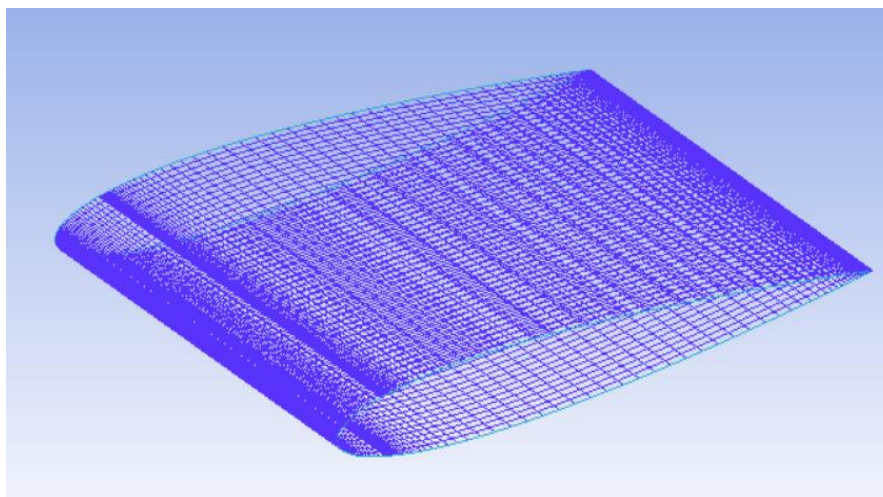

Figure 8: 3D view of the mesh of baseline airfoil isolated in ICEM CFD

The size of the mesh was found to be:

```
Mesh size:
     NODES = 2470000
     QUADS = 146224
     HEXAS = 2396394
```

Figure 9: Size of the mesh

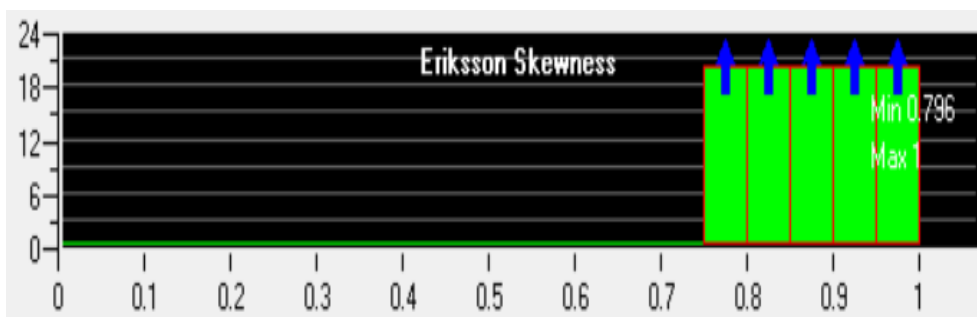The Eriksson Skewness of the mesh was found to be:

Figure 10: Eriksson Skewness of the mesh

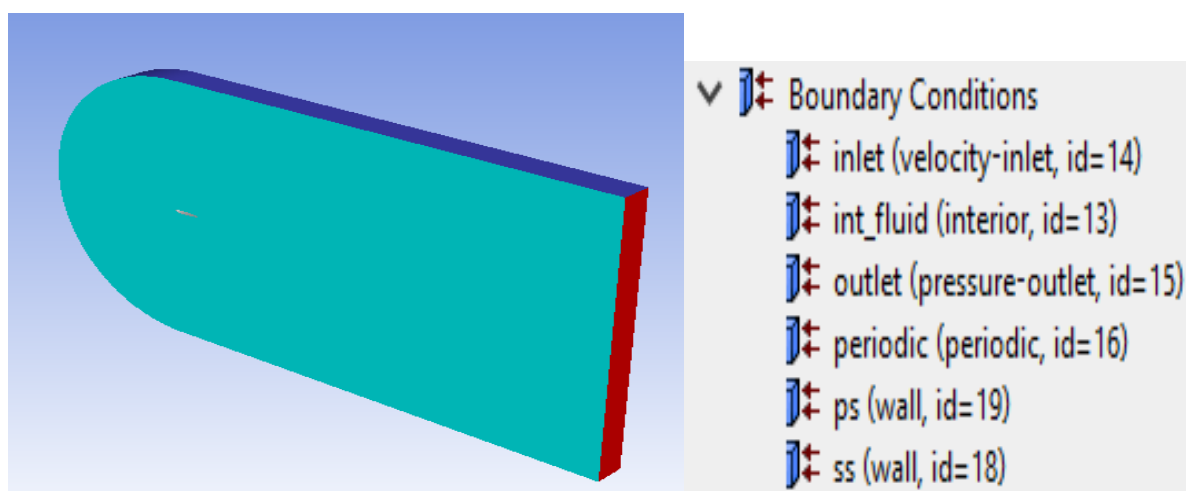The boundary conditions applied in ANSYS Fluent were:

Figure 11: Boundary conditions of the mesh in ANSYS Fluent

From Figure 11, we observed that the inlet boundary condition was represented by a dark blue colour surface with a velocity inlet condition, the outlet boundary condition was represented by a red colour surface with a pressure inlet condition, side walls were represented by light blue colour with periodic boundary condition and the upper surface of the airfoil (SS or Suction Surface) and the lower surface of airfoil (PS or Pressure Surface) were represented by wall boundary condition.

The Y-Plus value of the mesh was found to be:

Figure 12: Y-Plus value of the mesh

Therefore, the characteristics of mesh and boundary conditions were of high quality.

After simulating in ANSYS Fluent for higher iterations, we get the following comparison between the results of the experiment and the simulation:

Table 12: Comparison of CL at various α (between Experiment and Simulation)

α	CL (Experiment)	CL (3D CFD Simulation)
1	0.05	0.03
2	0.19	0.15
3	0.3	0.27
4	0.405	0.38
5	0.525	0.48
6	0.605	0.57
7	0.675	0.65
8	0.775	0.75
9	0.81	0.83
10	0.9	0.92
11	0.95	0.97
12	0.85	0.92
13	0.775	0.75
14	0.7	0.68
15	0.65	0.63
16	0.625	0.61
18	0.6125	0.59
20	0.6125	0.6
21	0.625	0.61
22	0.7	0.68
24	0.75	0.78

Table 13: Comparison of CD at various α (between Experiment and Simulation)

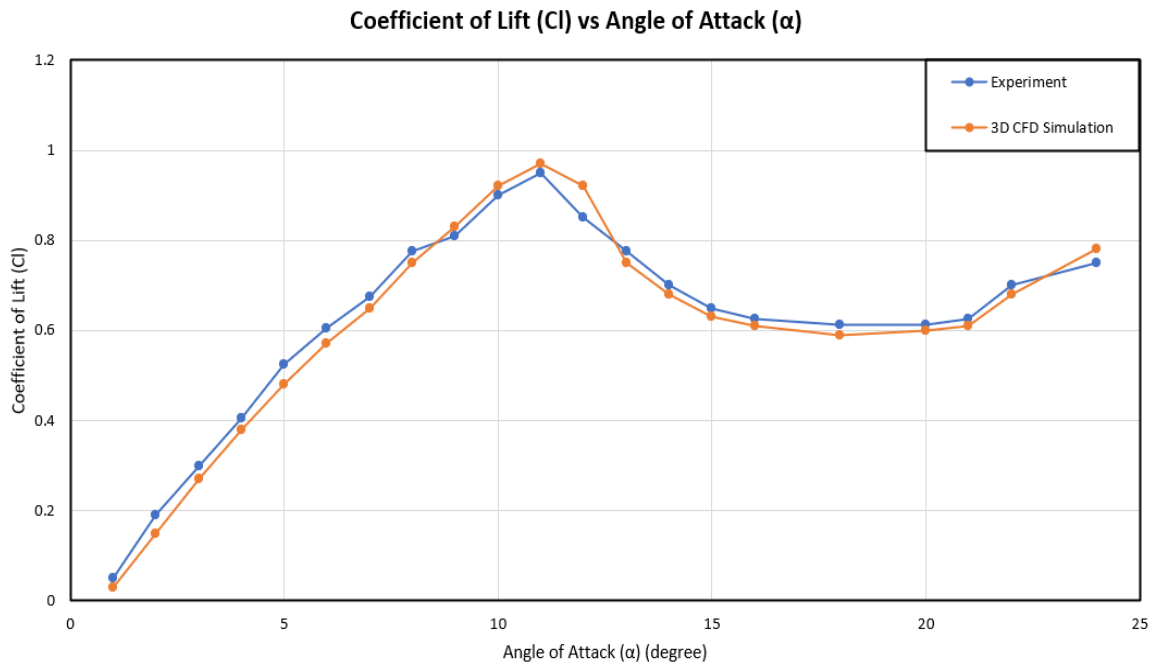| Angle of Attack (α)	CD (Experiment)	CD (3D CFD Simulation)
1	0.01	0.005
2	0.01	0.005
3	0.01	0.005
4	0.01	0.005
5	0.015	0.006
6	0.015	0.007
7	0.015	0.008
8	0.02	0.009
9	0.02	0.014
10	0.02	0.02
11	0.04	0.03
12	0.055	0.04
13	0.085	0.06
14	0.125	0.1
15	0.19	0.16
16	0.21	0.2
17	0.23	0.22
18	0.25	0.24
19	0.275	0.27
20	0.3	0.32

After plotting, we get:

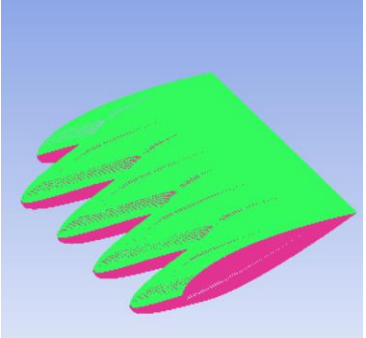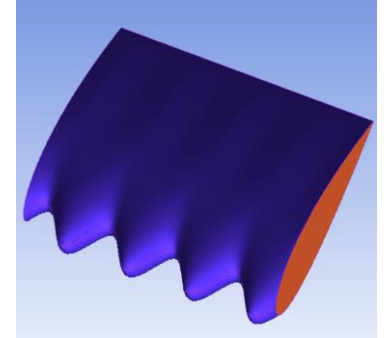**Figure 13: Plot of CL vs α (between Experiment and Simulation)**
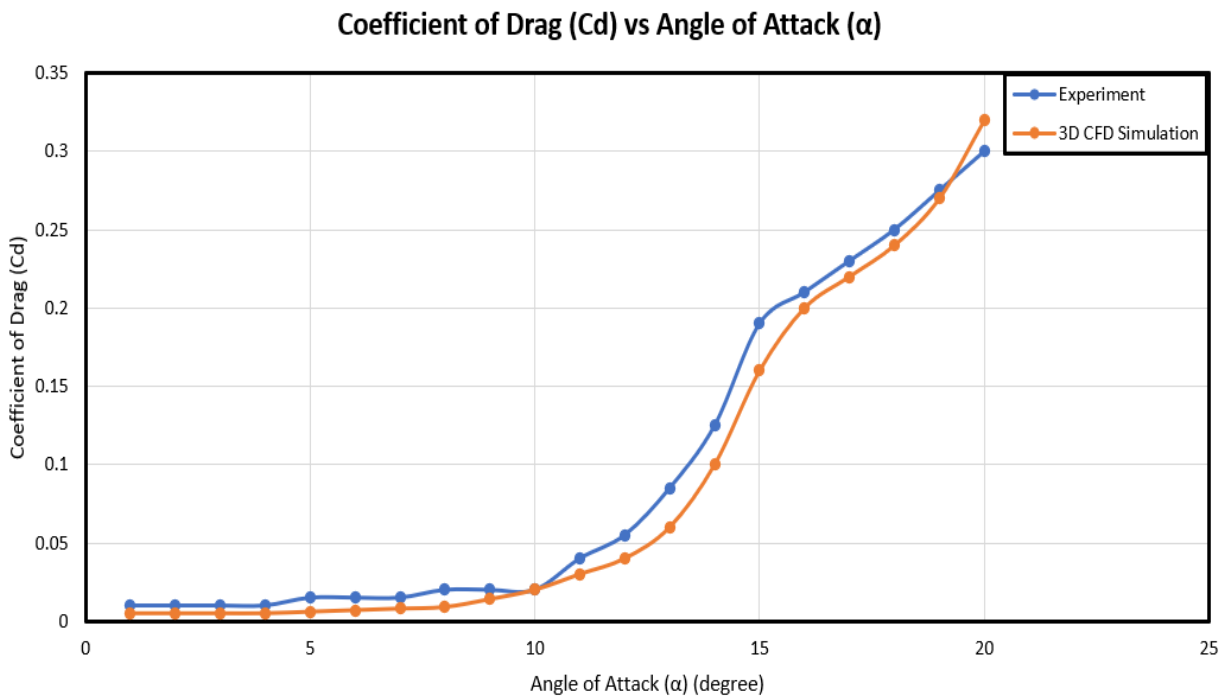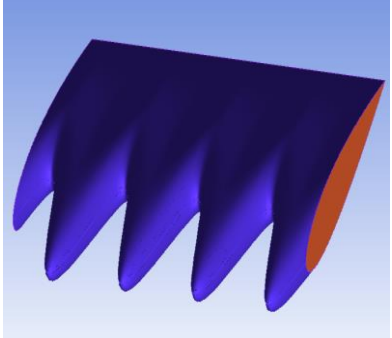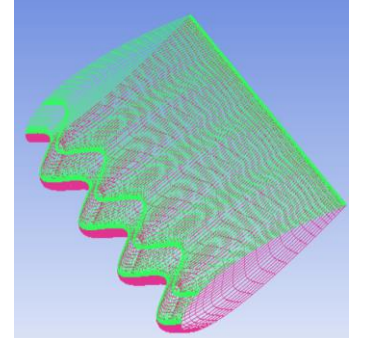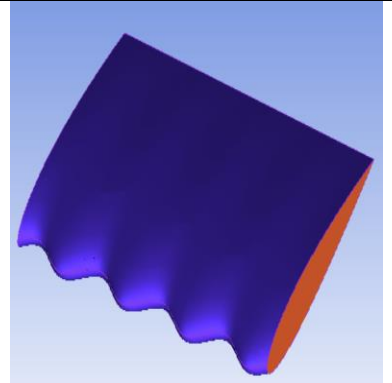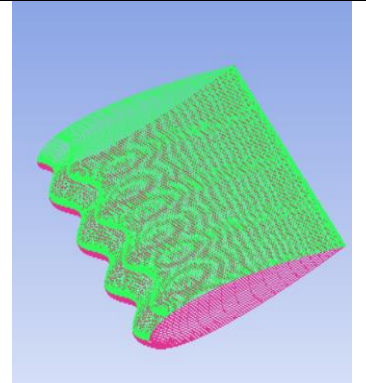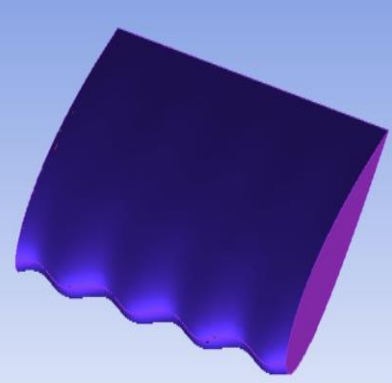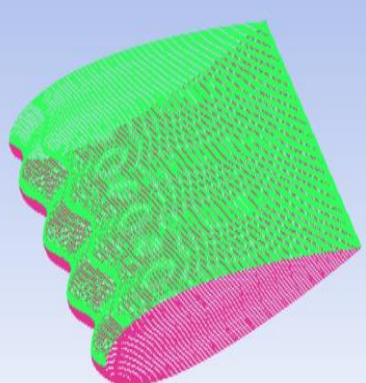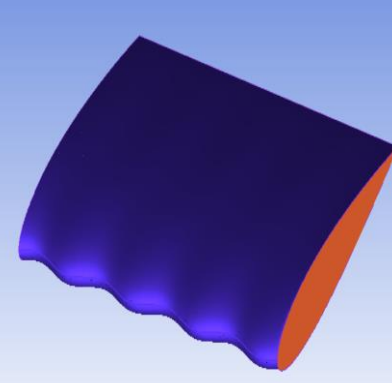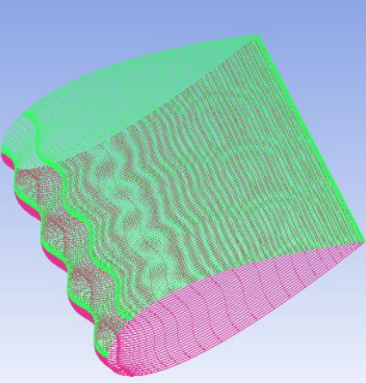
Figure 14: Plot of CD vs α (between Experiment and Simulation)

It was observed that the lift and drag characteristics obtained in our analysis were comparable (as shown in the graphs of CL versus α and CD versus α) to those obtained by experimental method of Winslow et. al [32], thereby validating our method of simulation.

CFD analysis of baseline 3D airfoil and airfoil with tubercles

From the results of XFOIL analysis, NACA 0012 was selected. Since, XFOIL used a default chord length of 1 m, hence we used the same airfoil that we chose for validation and so the same mesh. The geometry and meshing of the airfoils with tubercles using ICEM CFD is shown in Table 14.

Table 14: Geometry and meshing of airfoils using ICEM CFD

p/c	p/A	Geometry of airfoil using ICEM CFD	Meshing of airfoil using ICEM CFD
0.25	1		
0.25	3		
0.25	6		
0.25	9		
0.25	12		

Using the same procedure that was implemented for validation but changing Reynolds number to 50000 (as selected for XFOIL analysis), we got the following results:

Table 15: CFD Analysis results for 3D baseline NACA 0012 airfoil

α (Degree)	CL	CD	L/D
0	0	0.021	0
1	-0.03	0.022	-1.41
2	0.21	0.025	8.35
3	0.45	0.023	19.47
4	0.55	0.023	23.75
5	0.62	0.024	25.46
6	0.7	0.028	24.61
7	0.77	0.034	22.54
8	0.83	0.044	19.01
9	0.84	0.059	14.4
10	0.66	0.098	6.71
11	0.59	0.133	4.47
12	0.62	0.148	4.16
13	0.62	0.161	3.87
14	0.64	0.174	3.67
15	0.69	0.194	3.58
16	0.7	0.203	3.45

Table 16: CFD Analysis results for tubercled airfoil with p/c=0.25 and p/A=1

α (Degree)	CL	CD	L/D
0	0	0.018	0
1	-0.02	0.019	-1.05876
2	0.27	0.022	12.40239
3	0.5	0.020	24.53386
4	0.6	0.020	29.95507
5	0.68	0.021	31.65736
6	0.745	0.025	29.45828
7	0.82	0.031	26.13129
8	0.88	0.041	21.50012
9	0.91	0.056	16.36396
10	0.63	0.101	6.217923
11	0.56	0.136	4.122194
12	0.58	0.151	3.837248
13	0.59	0.164	3.600635
14	0.61	0.177	3.442049
15	0.66	0.197	3.35417
16	0.67	0.206	3.257329

Table 17: CFD Analysis results for tubercled airfoil with p/c=0.25 and p/A=3

α (Degree)	CL	CD	L/D
0	0	0.015	0
1	0	0.016	0
2	0.3	0.019	15.98295
3	0.56	0.017	32.22094
4	0.65	0.017	38.16794
5	0.72	0.018	38.96104
6	0.79	0.022	35.4419
7	0.85	0.028	29.95067
8	0.91	0.038	23.99156
9	0.94	0.053	17.86733
10	0.61	0.104	5.847393
11	0.54	0.139	3.889089
12	0.56	0.154	3.632825
13	0.57	0.167	3.416037
14	0.59	0.180	3.273776
15	0.64	0.200	3.203684
16	0.65	0.209	3.114668

Table 18: CFD Analysis results for tubercled airfoil with p/c=0.25 and p/A=6

α (Degree)	CL	CD	L/D
0	0	0.006	0
1	0.05	0.007	7.256894
2	0.37	0.010	37.87103
3	0.63	0.008	75.179
4	0.72	0.008	89.66376
5	0.79	0.009	83.33333
6	0.86	0.013	64.71031
7	0.92	0.019	47.47162
8	0.98	0.029	33.87487
9	1.01	0.044	23.15983
10	1.02	0.083	12.24196
11	0.47	0.148	3.178898
12	0.49	0.163	3.003371
13	0.5	0.176	2.843171
14	0.52	0.189	2.748124
15	0.57	0.209	2.730277
16	0.58	0.218	2.664339

Table 19: CFD Analysis results for tubercled airfoil with p/c=0.25 and p/A=9

α (Degree)	CL	CD	L/D
0	0	0.009	0
1	0.03	0.010	3.033367
2	0.34	0.013	26.6249
3	0.6	0.011	52.72408
4	0.69	0.011	62.55666
5	0.75	0.012	60.09615
6	0.82	0.016	50.33763
7	0.88	0.022	39.32082
8	0.94	0.032	29.4394
9	0.97	0.047	20.81098
10	0.98	0.086	11.3531
11	0.5	0.145	3.451847
12	0.52	0.160	3.246956
13	0.53	0.173	3.066065
14	0.55	0.186	2.953496
15	0.6	0.206	2.915877
16	0.61	0.215	2.841306

Table 20: CFD Analysis results for tubercled airfoil with p/c=0.25 and p/A=12

α (Degree)	CL	CD	L/D
0	0	0.012	0
1	0.01	0.013	0.775795
2	0.32	0.016	20.29169
3	0.58	0.014	40.3338
4	0.67	0.014	47.75481
5	0.73	0.015	47.15762
6	0.8	0.019	41.47227
7	0.86	0.025	33.88495
8	0.92	0.035	26.33839
9	0.95	0.050	19.14937
10	0.96	0.089	10.74787
11	0.52	0.142	3.665844
12	0.54	0.157	3.436207
13	0.55	0.170	3.237961
14	0.57	0.183	3.111014
15	0.62	0.203	3.057652
16	0.63	0.212	2.97605

Recommendation of the arrived specifications of tubercle for the given application

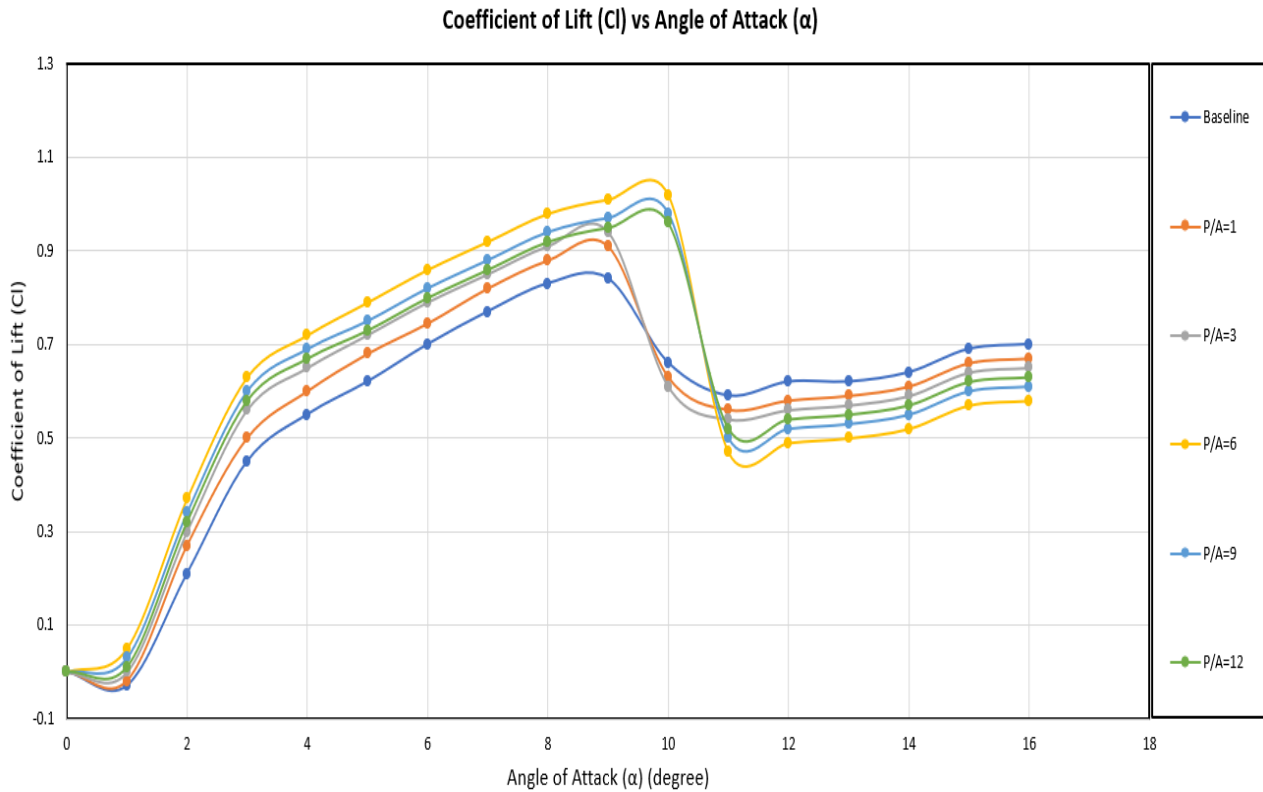Plotting the results of simulations of various airfoils, we get:

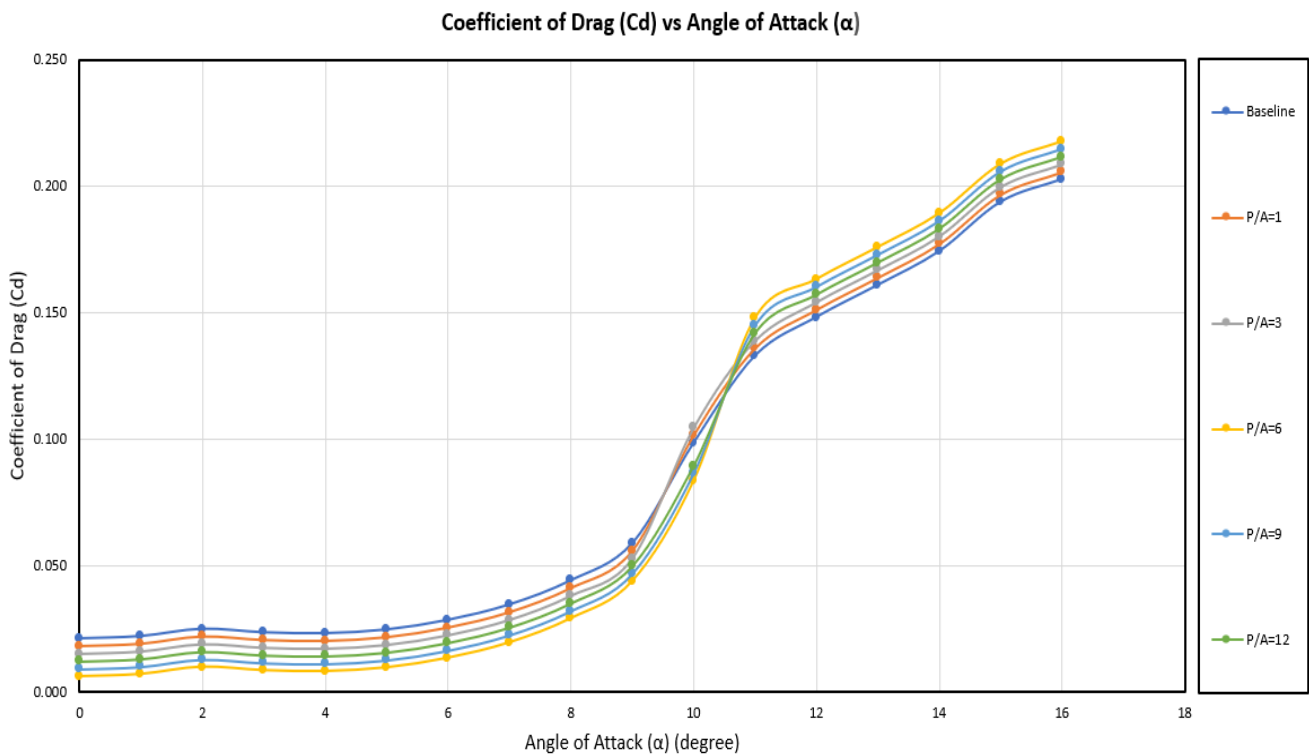**Figure 15: CL vs α for baseline and tubercled airfoils**

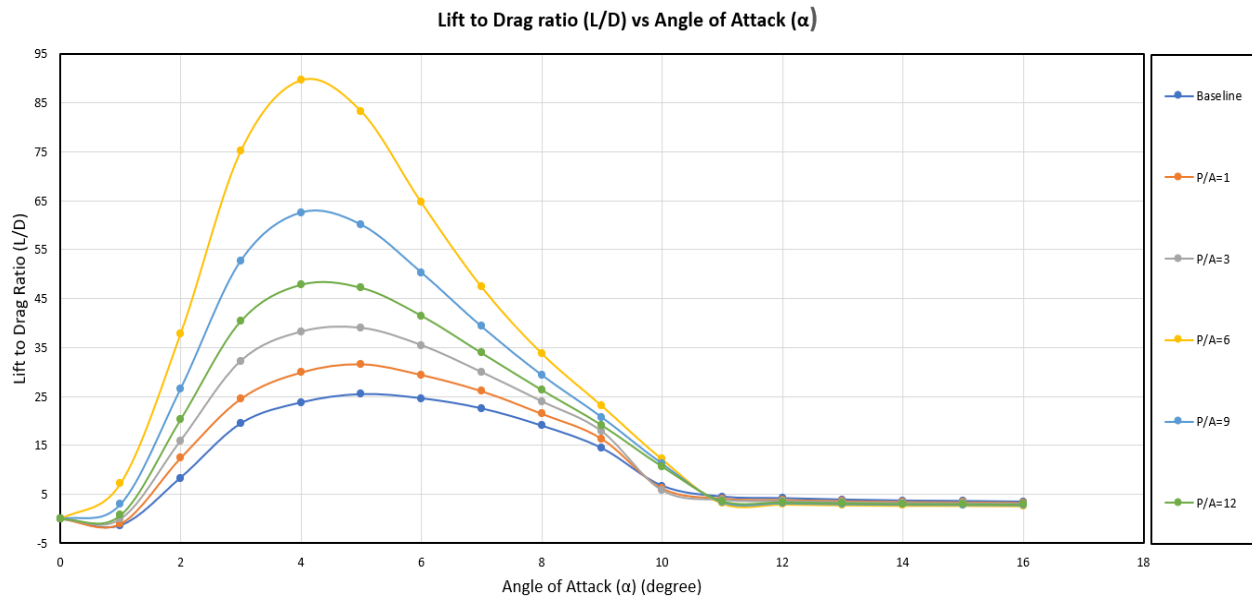**Figure 16: CD vs α for baseline and tubercled airfoils**

Figure 17: L/D vs α for baseline and tubercled airfoils

From the above figures, we observed that the L/D and CL of a tubercled airfoil with p/A of 6 had the best aerodynamic performance compared to any other airfoil. Hence, it was recommended to use a tubercled airfoil of p/A of 6 for low-speed wind turbine application.

DISCUSSIONS

The effects of the cutting-edge tubercles on the aerodynamics of the blades of wind turbines are fascinating in terms of their effectiveness and potential. Among the airfoils we investigated, we found that the NACA 0015 had the highest CL at a stall angle of 9 degrees (which was superior to the other airfoils), and lift reduced as stall angle increased across the NACA series [33]. This result agrees with what was found by other investigators, who also revealed the higher aerodynamic stability of cutting-edge modifications that induce a vortex to boost lift after a stall [34].

Our measurements showed early stall for the NACA 0005 airfoil at just 3 degrees, supporting other research that indicates lead edge modifications can effectively prevent separation of flow and therefore postpone stall [35]. We made similar observations, where tubercles reduced the early stall effects for various designs, indicating that they were effective in preventing lift loss. Stall delay is critical to the performance of wind turbines, especially when they are running in unstable conditions.

Impaired drag plays a critical role in lift, with induced drag increasing drag after high lift following a stall (our study observed). It is an established feature of aerodynamics, where drag from lift becomes important, and hence design optimization is needed. This finding aligns with studies that reported these shifts in drag over lift in tubercled airfoils and helped explain the role of design in performance parameters.

As for CDs, we found a negative trend between pre-stall and post-stall, due to the increasing airfoil thickness, and a negative trend towards post-stall. This result aligns with recent studies that indicate heavier airfoils typically have lower CD in flight, although stall transition has its own effect, depending on design [36]. These kinds of subtle effects illustrate how thickness and shape are critical to aerodynamic efficiency.

The higher L/D values for NACA 0012 and 0011 suggest superior performance, which is consistent with other reports pointing to the relative benefits of certain airfoil designs, particularly in terms of turbine efficiencies. Our decision to select NACA 0012 based on optimal L/D performance reinforces prior recommendations that efficient turbine design requires an optimal balance of aerodynamic and structural performance with the use of smart airfoils.

Lastly, the effectiveness of our simulation approaches (XFOIL analysis and CFD validation) in line with the literature is that the computing systems are able to simulate airfoil performance well for early small wind turbine designs. Preliminary research has been similar in the same regard to the validity of computational simulations to predict aerodynamic properties against experimental data [37]. Further, the improved performance at p/A ratio 6 for tubercled designs is consistent with results that specified optimal p/A ratios for better performance in low-speed environments [35].

CONCLUSION

To conclude, the present investigation revealed NACA 0015 had the highest CL at stall angle of 9 degrees and early stalling by NACA005 at 3 degrees. The drag increased with an increase in lift even after stalling because of the phenomenon known as "induced drag". In pre-stall, the CD showed a decline with a decrease in thickness from NACA 0025 to NACA 0005, and in post-stall, the CD showed a reverse effect. The L/Ds of NACA 0012 and 0011 were higher than that of other airfoils. NACA 0012 was chosen as it had the best L/D compared to other airfoils. Comparison of the data from simulated airfoil and experimental results indicated that the simulation procedure was adequate for predicting the aerodynamic performance and performing preliminary design of small wind turbines. From the simulation of tubercles of different p/As and comparison of the aerodynamic performances of the baseline airfoil versus the tubercled airfoil, p/A of 6 was obtained to provide the best performance for low-speed wind turbine application.

More in-depth research on the application of tubercle technology to wind turbine aerodynamics is required as the goal of wind energy research is to help the technological development of new environmentally friendly and cost-effective wind energy systems. In future simulations, the airfoil can be expanded to have at least 6 tubercles, instead of having only four tubercles as in the present study. In the future, it would be worth modeling an airfoil more closely resembling a humpback flipper. Also, other mechanisms for performance enhancement such as the generation of streamwise vortices, which improve momentum exchange in the boundary layer can be investigated.

REFERENCES

[1] Shen, W. Z. (2019). Special issue on wind turbine aerodynamics. *Applied Sciences*, *9*(9), 1–4. https://doi.org/10.3390/app9091725

[2] Zhu, M., Yu, Y., Zhu, J., Zhang, J., Gao, Q., Li, H., Zhang, Y., Wang, Z. L., & Cheng, T. (2023). Bionic Blade Lift-Drag Combination Triboelectric-Electromagnetic Hybrid Generator with Enhanced Aerodynamic Performance for Wind Energy Harvesting. *Advanced Energy Materials*, *13*(46), 2303119. https://doi.org/10.1002/aenm.202303119

[3] Roy, P., He, J., Zhao, T., & Singh, Y. V. (2022). Recent Advances of Wind-Solar Hybrid Renewable Energy Systems for Power Generation: A review. *IEEE Open Journal of the Industrial Electronics Society*, *3*, 81–104. https://doi.org/10.1109/ojies.2022.3144093

[4] Salles, A. O. T., Santos, L. T. D., & Campos, A. F. (2019). Consolidation of the wind energy sector in the Brazilian electricity matrix: opportunities, advantages and challenges. *International Journal of Innovation and Sustainable Development*, *13*(3/4), 392–409. https://doi.org/10.1504/ijisd.2019.100424

[5] Wan, C., Lin, J., Wang, J., Song, Y., & Dong, Z. Y. (2017). Direct quantile regression for nonparametric probabilistic forecasting of wind power generation. *IEEE Transactions on Power Systems*, *32*(4), 2767–2778. https://doi.org/10.1109/tpwrs.2016.2625101

[6] Da Rocha, L. F., Brandao, D. I., De S Medeiros, K., Dall'asta, M. S., & Lazzarin, T. B. (2023). Coordinated decentralized control of dynamic Volt-VAR function in oil and gas platform with wind power generation. *IEEE Open Journal of Industry Applications*, *4*, 269–278. https://doi.org/10.1109/ojia.2023.3307299

[7] Chen, H., Zuo, Y., Chau, K. T., Zhao, W., & Lee, C. H. T. (2021). Modern electric machines and drives for wind power generation: A review of opportunities and challenges. *IET Renewable Power Generation*, *15*(9), 1864–1887. https://doi.org/10.1049/rpg2.12114

[8] Herbert, G. M. J., Iniyan, S., Sreevalsan, E., & Rajapandian, S. (2007). A review of wind energy technologies. *Renewable and Sustainable Energy Reviews*, *11*(6), 1117–1145. https://doi.org/10.1016/j.rser.2005.08.004

[9] Chen, Z., & Blaabjerg, F. (2006). Wind Energy: The World's Fastest Growing Energy Source. *IEEE Power Electronics Society Newsletter*, *18*(3), 15–19. https://ewh.ieee.org/soc/pels/pdf/pelsNL0306.pdf

[10] Li, H., & Chen, Z. (2008). Overview of different wind generator systems and their comparisons. *IET Renewable Power Generation*, *2*(2), 123–138. https://doi.org/10.1049/iet-rpg:20070044

[11] Ng, B. F., New, T. H., & Palacios, R. (2016). Effects of leading-edge tubercles on wing flutter speeds. *Bioinspiration & Biomimetics*, *11*(3), 036003. https://doi.org/10.1088/1748-3190/11/3/036003

[12] Zhao, M., Zhang, M., & Xu, J. (2017). Numerical simulation of flow characteristics behind the aerodynamic performances on an airfoil with leading edge protuberances. *Engineering Applications of Computational Fluid Mechanics*, *11*(1), 193–209. https://doi.org/10.1080/19942060.2016.1277165

[13] Weber, P. W., Howle, L. E., & Murray, M. M. (2010). Lift, drag, and cavitation onset on rudders with leading-edge tubercles. *Marine Technology and SNAME News*, *47*(01), 27–36. https://doi.org/10.5957/mtsn.2010.47.1.27

[14] Rostamzadeh, N., Kelso, R. M., Dally, B. B., & Tian, Z. F. (2012). An Experimental and Computational Study of Flow over a NACA 0021 Airfoil with Wavy Leading Edge Modification. *18th Australasian Fluid Mechanics Conference*, 1–4. https://flair.monash.edu/intranet/proceedings/18afmc/Documents/55%20-%20Rostamzadeh.pdf

[15] Osei, E. Y., Opoku, R., Sunnu, A. K., & Adaramola, M. S. (2020). Development of high performance airfoils for application in small wind turbine power generation. *Journal of Energy*, *2020*(1), 9710189. https://doi.org/10.1155/2020/9710189

[16] Johari, H., Henoch, C., Custodio, D., & Levshin, A. (2007). Effects of Leading-Edge protuberances on Airfoil performance. *AIAA Journal*, *45*(11), 2634–2642. https://doi.org/10.2514/1.28497

[17] Nazemian, A., & Ghadimi, P. (2020). Shape optimization of a hydrofoil with leadingedge protuberances using full factorial sweep sampling and an RBF surrogate model. *Zeszyty Naukowe Akademii Morskiej W Szczecinie*, *62*(134), 116–123. https://doi.org/10.17402/426

[18] Rohmawati, I., Arai, H., Nakashima, T., Mutsuda, H., & Doi, Y. (2020). Effect of wavy leading edge on pitching rectangular wing. *Journal of Aero Aqua Bio-mechanisms*, *9*(1), 1–7. https://doi.org/10.5226/jabmech.9.1

[19] Singh, R. K., Ahmed, M. R., Zullah, M. A., & Lee, Y.-H. (2012). Design of a low Reynolds number airfoil for small horizontal axis wind turbines. *Renewable Energy*, *42*, 66–76. https://doi.org/10.1016/j.renene.2011.09.014

[20] Ng, B. F., Ong, E. J. G., Palacios, R., & New, T. H. (2020). Effects of Leading-Edge tubercles on structural dynamics and aeroelasticity. In D. T. H. New & B. F. Ng (Eds.), *Flow Control Through Bio-inspired Leading-Edge Tubercles* (pp. 147–173). https://doi.org/10.1007/978-3-030-23792-9_7

[21] Miklosovic, D. S., Murray, M. M., Howle, L. E., & Fish, F. E. (2004). Leading-edge tubercles delay stall on humpback whale (Megaptera novaeangliae) flippers. *Physics of Fluids*, *16*(5), L39–L42. https://doi.org/10.1063/1.1688341

[22] Rehman, S., Alam, M. M., Alhems, L. M., & Rafique, M. M. (2018). Horizontal Axis Wind Turbine Blade Design Methodologies for Efficiency Enhancement—A Review. *Energies*, *11*(3), 1–34. https://doi.org/10.3390/en11030506

[23] Lohry, M. W., Clifton, D., & Martinelli, L. (2012). Characterization and Design of Tubercle Leading-Edge Wings. *Seventh International Conference on Computational Fluid Dynamics (ICCFD7)*, 1–11. https://www.iccfd.org/iccfd7/assets/pdf/papers/ICCFD7-4302_paper.pdf

[24] Shi, W., Atlar, M., Seo, K., Norman, R., & Rosli, R. (2016). Numerical Simulation of a Tidal Turbine Based Hydrofoil With Leading-Edge Tubercles. *Proceedings of the ASME 2016 35th International Conference on Ocean, Offshore and Arctic Engineering*, *6*, V006T09A005. https://doi.org/10.1115/omae2016-54796

[25] Lu, Y., Li, Z., Chang, X., Chuang, Z., & Xing, J. (2021). An aerodynamic optimization design study on the bio-inspired airfoil with leading-edge tubercles. *Engineering Applications of Computational Fluid Mechanics*, *15*(1), 292–312. https://doi.org/10.1080/19942060.2020.1856723

[26] Rao, B. R., & Sahitya, R. (2015). Numerical And Experimental Investigation of The Flow Field Around NACA 0012 Aerofoil. *International Journal on Theoretical and Applied Research in Mechanical Engineering (IJTARME)*, *4*(4), 18–26. https://www.irdindia.in/journal_ijtarme/pdf/vol4_iss4/3.pdf

[27] Gawad, A. F. A. (2013). Utilization of Whale-Inspired Tubercles as a Control Technique to Improve Airfoil Performance. *Transaction on Control and Mechanical Systems*, *2*(5), 212–218. https://www.academia.edu/download/33338078/Whale-Inspired-Tubercles.pdf

[28] Chen, J.-H., Li, S.-S., & Nguyen, V. T. (2012). THE EFFECT OF LEADING EDGE PROTUBERANCES ON THE PERFORMANCE OF SMALL ASPECT RATIO FOILS. *15th International Symposium on Flow Visualization*, 1–16. https://typeset.io/pdf/the-effect-of-leading-edge-protuberances-on-the-performance-4sq8lzwkgl.pdf

[29] Joseph, J., & Sathyabhama, A. (2020). Numerical Study on the Effect of Leading Edge Tubercle on Symmetrical Airfoil at Low Reynolds Number. *The International Journal of Engineering and Science (IJES)*, 65–71. https://www.theijes.com/papers/NHTFF-2020/Volume%20-3/9,%2065-71.pdf

[30] Fish, F. E., Weber, P. W., Murray, M. M., & Howle, L. E. (2011). The Tubercles on Humpback Whales' Flippers: Application of Bio-Inspired Technology. *Integrative and Comparative Biology*, *51*(1), 203–213. https://doi.org/10.1093/icb/icr016

[31] Yan, Y., Avital, E., Williams, J., & Cui, J. (2021). Aerodynamic performance improvements of a vertical axis wind turbine by leading-edge protuberance. *Journal of Wind Engineering and Industrial Aerodynamics*, *211*, 104535. https://doi.org/10.1016/j.jweia.2021.104535

[32] Winslow, J., Otsuka, H., Govindarajan, B., & Chopra, I. (2018). Basic understanding of Airfoil characteristics at Low Reynolds numbers (104–105). *Journal of Aircraft*, *55*(3), 1050–1061. https://doi.org/10.2514/1.c034415

[33] Yirijor, J., & Siaw-Mensah, N. A. (2023). Design and optimisation of horizontal axis wind turbine blades using biomimicry of whale tubercles. *Journal of Engineering Research and Reports*, *25*(5), 100–112. https://doi.org/10.9734/jerr/2023/v25i5915

[34] Thomas, E., Kumar, V. V., VD, D., Lal, N. S., & Shah, D. A. (2017). Computational analysis on application of tubercles for the performance improvement of horizontal axis wind turbine. *Manufacturing Science and Technology*, *4*(3), 35–42. https://doi.org/10.13189/mst.2017.040301

[35] Ke, W., Hashem, I., Zhang, W., & Zhu, B. (2022). Influence of leading-edge tubercles on the aerodynamic performance of a horizontal-axis wind turbine: A numerical study. *Energy*, *239*, 1–17. https://doi.org/10.1016/j.energy.2021.122186

[36] Chen, T., Jiang, X., Wang, H., Li, Q., Li, M., & Wu, Z. (2020). Investigation of leading-edge slat on aerodynamic performance of wind turbine blade. *Proceedings of the Institution of Mechanical Engineers, Part C: Journal of Mechanical Engineering Science*, *235*(8), 1329–1343. https://doi.org/10.1177/0954406220941883

[37] Tian, F.-B. (2021). Numerical simulations of biological flows and their engineering applications. *Proceedings of the Institution of Mechanical Engineers, Part C: Journal of Mechanical Engineering Science*, *235*(2), 205–207. https://doi.org/10.1177/0954406220969095

Cite this Article